UKAEA FUS 389

UKAEA Fusion
(EURATOM/UKAEA Fusion Association,
Culham Science Centre)

Overview of ECRH Experiments

Brian Lloyd

July 1998

Invited paper presented at the 2nd Europhysics Topical Conference on Radiofrequency Heating and Current Drive of Fusion Devices, Brussels 1998 - to be published in Plasma Physics & Controlled Fusion.

UKAEA Fusion

Culham Science Centre, Abingdon
Oxfordshire OX14 3DB
United Kingdom
Telephone 01235 463325
Facsimile 01235 464192

OVERVIEW OF ECRH EXPERIMENTAL RESULTS

Brian Lloyd

UKAEA Fusion, Culham Science Centre, Abingdon, OX14 3DB, UK
(UKAEA/Euratom Fusion Association)

Abstract

A review of the present status of electron cyclotron heating and current drive experiments in toroidal fusion devices is presented. In addition to basic heating and current drive studies the review also addresses advances in wave physics and the application of electron cyclotron waves for instability control, transport studies, preionisation/start-up assist, etc. A comprehensive overview is given with particular emphasis on recent advances since the major review of Erckmann and Gasparino 1994, including results from the latest generation of high power, high frequency experiments.

1. Introduction

Electron Cyclotron Resonance Heating (ECRH) is a highly efficient, flexible, localised and controllable heating scheme for which the physics of wave propagation and absorption is reasonably well-understood. The location of the power deposition in toroidal devices may be controlled by adjustment of the toroidal field or by poloidal and/or toroidal steering of the launched beam at fixed magnetic field. In addition, recent advances in the development of frequency tuneable sources offer further flexibility. Transmitted power measurements and power deposition studies in a number of devices have confirmed the predictions of linear wave absorption theory. Furthermore, in recent years, the installation of high frequency ECRH systems with good beam focusing and steerability has led to the confirmation of rather subtle aspects of the theory (Section 2). Sophisticated codes have been developed, which accurately describe present experiments and provide a reliable predictive capability for future devices.

Effective plasma heating has been demonstrated over many years in mirrors, tokamaks and stellarators and reliable access to modes with improved confinement, like the so-called H-mode, is achieved in present day devices. Plasmas with negative central shear have been established by off-axis ECRH. Electron cyclotron current drive (ECCD) has been demonstrated in both tokamaks and stellarators with an efficiency which is generally observed to be in good agreement with theoretical predictions. The localised nature of the wave-plasma interaction has been exploited to good effect for local transport studies and for the control of various instabilities occurring in tokamak plasmas including sawteeth, tearing modes, locked modes and ELMs. The flexibility of electron cyclotron systems, including the capability to modulate the source power at high frequency, has allowed sophisticated instability feedback control applications to be investigated. ECRH preionisation and assisted start-up is an established and robust technique which has been demonstrated in a large number of tokamaks and ECRH is employed routinely for plasma production in stellarators. ECRH discharge cleaning is one of the wall conditioning methods being considered for ITER. The effectiveness of ECRH discharge cleaning has been demonstrated in a number of devices (Jotaki and Itoh 1997 and references therein).

The properties of electron cyclotron wave absorption and propagation make electron cyclotron heating and current drive an attractive scheme for Next Step devices such as ITER. Strong single pass damping is expected and electron cyclotron waves have the potential to provide significant current drive capability, both in the core and off-axis. Furthermore, there is no damping on alpha particles and the ECRH power densities encountered in ITER are much less than those estimated to be necessary for non-linear effects to set in (Harvey *et al* 1997). Electron cyclotron systems also possess a number of attractive technological features for present and Next Step devices. Since the waves propagate in vacuum, the launcher does not have to be in close proximity to the plasma and there are no requirements on plasma edge control. As a result, no specific impurity generation problems have generally been encountered, even at heating power densities far in excess of those that might be employed in Next Step devices. High power densities can be transmitted at the antenna, for example allowing 50MW to be injected through a single ITER port if necessary.

Several review papers on ECRH have been published in the recent past (e.g. Prater 1990, Alikaev *et al* 1992a, Erckmann and Gasparino 1994). The present brief overview will attempt to summarise the status of ECRH experiments in toroidal devices with special emphasis on recent advances since the rather comprehensive review of Erckmann and Gasparino, including results from the latest generation of high power experiments just reaching fruition. The status of ECRH technology is being reviewed by Tran 1998.

2. Advances in Basic Physics

Two mechanisms are responsible for electron cyclotron absorption (Bornatici *et al* 1983):

- the interaction of an elliptically polarised electric field rotating in the same direction as electrons with a frequency close to the electron gyrofrequency or one of its harmonics,
- the Lorentz force arising from the interaction of the parallel (to the static magnetic field) electron velocity with the wave magnetic field.

The resonance condition for the lth harmonic is,

$$\omega - k_{\|} v_{\|} = l \omega_{ce}/\gamma \qquad (1)$$

where ω_{ce} is the cyclotron frequency, γ is the relativistic mass factor, $k_{\|}$ is the parallel wavenumber and $v_{\|}$ is the parallel velocity. Note that equation (1) may be satisfied for $\omega > l\omega_{ce}$ (upshifted absorption) or $\omega < l\omega_{ce}$ (downshifted absorption). Electron cyclotron wave propagation and absorption is generally well-described by linear theory. Direct measurements of power transmitted through the plasma in a single pass are usually in good agreement with ray tracing calculations. Such measurements reflect not only the resonant absorption but also non-resonant losses (e.g. refraction, scattering) which can be identified by operation at a non-resonant magnetic field. Refraction losses can be significant (van Gelder *et al* 1997) but scattering by edge density turbulence typically reduces the power in the beam by only a few per cent (van Gelder *et al* 1997, Roberts 1995). Refraction and absorption measurements for central ordinary mode (OM) heating at the fundamental resonance in RTP (Smits *et al* 1992) and also in TEXT-U (Roberts 1995) are in good agreement with theory except for densities close to cutoff.

In RTP during high power ECRH (fundamental OM, low-field-side (LFS) injection), at low density, the electron cyclotron absorption (ECA) diagnostic exhibits asymmetric absorption with respect to the toroidal launch angle which is attributed to superthermal electrons accelerated by the dc electric field (Peeters *et al* 1995). The experimental observations are reproduced by Fokker-Planck calculations and confirm the upshifted/downshifted nature of the cyclotron resonance interaction for energetic electrons. Upshifted/downshifted electron cyclotron absorption has been demonstrated in many ECRH experiments and has also been observed in combined ECRH + LHCD (lower hybrid current drive) experiments in JFT-2M (Kawashima *et al* 1991) and WT-3 (Tanaka *et al* 1992).

Specific experiments were performed in Tore-Supra (Segui *et al* 1996) to measure the optical thickness of the 3rd harmonic extra-ordinary mode (XM) for vertical propagation, i.e. the direction of constant cyclotron frequency, over the full frequency spectrum. For frequencies above and below the resonant range the signal level is

determined by refraction. Comparison of the data with ray tracing/absorption calculations provided a direct validation of linear relativistic theory. Furthermore, at low plasma currents the spectra exhibited a peak close to $3\omega_{ce}$ on the high frequency side of the resonance which could be attributed to hot plasma corrections to the real part of the refractive index which affect the ray propagation.

The agreement of the measured electron cyclotron absorption with theory is sufficiently robust that ECA has become an established diagnostic technique (Segui and Giruzzi 1994, Segui *et al* 1995, van Gelder *et al* 1995, Giruzzi *et al* 1995, Boyd *et al* 1995, Michelot *et al* 1996) providing information not only on bulk plasma parameters but also on superthermal electron behaviour, for example during LHCD.

Transmitted power measurements give an indication of the single pass absorption. The total multi-pass absorption may be estimated from measurements of the rate of change of plasma stored energy at power turn-on or turn-off. Such measurements often indicate a total absorption somewhat less than predicted. The 'missing power' may be associated with changes in stored magnetic energy, power absorption by energetic electrons (if power transfer to the bulk occurs on a slow timescale or if the energetic electrons are lost), an immediate change in confinement etc. The ECRH power deposition profile may be derived from modulated ECRH experiments, but high modulation frequency is required in order to minimise transport effects (see section 3) and this in turn imposes significant demands on diagnostic resolution. This is especially true for the latest generation of high power, high frequency ECRH experiments with good beam focusing and steerability. The peak power deposition was measured to be in good agreement with modelling in ASDEX-U 140GHz (Leuterer *et al* 1997) and in DIII-D 110GHz experiments (Luce *et al* 1997) but in both cases it was not possible to measure the deposition profile accurately with the available diagnostic resolution. Estimates of the power deposition profile in FTU 140GHz experiments confirmed the very localised nature of the absorption (Cirant *et al* 1995). Due to the strong localised absorption, in this case, the local ECRH heating power density is 10 - 20 times higher than the ohmic one and during core heating of sawtoothing discharges this manifests itself as a dramatic change in the sawtooth slope (Fig 1).

Kinetic effects can be important in low-density high power ECRH discharges and the electron distribution function can depart significantly from Maxwellian. In the W7-AS stellarator the power deposition profile is estimated from the analysis of heat wave propagation stimulated by modulated ECRH (Rome *et al* 1997). In general, peaked deposition profiles, as predicted by a ray tracing code, are obtained but with an additional much broader contribution which is attributed to the radial transport of locally trapped superthermal electrons. The effect may be simulated using a convective Fokker-Planck model which simulates the radial ∇B drift of the toroidally trapped superthermal electrons generated by ECRH. When the broader component of power deposition is taken into account, no indication of 'missing power' was found. Note, in general, that a broadened deposition profile can also arise in devices in which the experimental conditions do not lead to single pass absorption. This is due to the fact that after multiple reflections, power may be resonantly absorbed at off-axis positions along the resonant layer.

Non-linear phenomena or parametric processes may be observed if the amplitude of the driving oscillation becomes large, for example in the vicinity of the upper hybrid resonance (UHR) where the electric field of the XM becomes strongly enhanced (Erckmann and Gasparino 1994 and references therein). In the MTX tokamak, where a 140GHz free electron laser was used to inject ultra high power pulses > 1GW for ~ 20ns, a reduction in absorption in accordance with non-linear theory was observed (Allen *et al* 1994).

Wave penetration is generally observed to be limited by the predicted cold plasma 'cutoffs', although for central densities above cutoff peripheral absorption may still be possible and can lead to efficient heating under some circumstances. A possibility for overcoming the density limit is the O-X-B conversion process proposed by Preinhaelter and Kopecky 1973. For propagation close to an optimum angle the obliquely launched OM converts to the XM in the vicinity of the OM cutoff, which then converts to an electron Bernstein wave (EBW) near the UHR. For the EBW, a density limit does not exist and it can propagate to the plasma centre where it is absorbed near the electron cyclotron resonance layer or in the non-resonant case (when the UHR fully encloses the plasma core) by collisional multiple pass damping. Efficient O-X-B heating at densities above the plasma cutoff was clearly demonstrated (Fig 2) for resonant and non-resonant fields in the stellarator W7-AS (Laqua *et al* 1997). Both the angular dependence of the OM→XM conversion (Fig 2b) and the parametric instability which typically accompanies XM→EBW conversion could be experimentally verified. This experiment represents an excellent test of hot plasma wave theory. The possibility of using the O-X-B conversion scheme in the spherical tokamak NSTX is being considered (Batchelor and Bigelow 1997).

3. Heating and Confinement

Effective electron cyclotron heating has been demonstrated in many devices. The localised and controllable nature of the absorption, together with the fact that initial energy transfer is exclusively to electrons, mean that ECRH is a well-known input quantity for transport investigations. In several respects, namely the power deposition on electrons, the absence of particle or momentum injection, and the potential for centrally peaked heating, ECRH resembles alpha particle heating. At high densities ions are heated by collisional energy transfer (Cirant *et al* 1996). Many devices exhibit a strong peaking of the electron temperature profile with on-axis ECRH, as indicated for example (Fig 3) in initial DIII-D 110GHz experiments (Chan *et al* 1997), indicating good local energy confinement in the core. Transport analyses of FTU plasmas, with high power density ECRH at 140GHz, in which high peak electron temperatures and very large temperature gradients up to 40keV/m were generated (Buratti *et al* 1995), showed that the electron thermal diffusivity was not worse than ohmic. Global energy confinement in ECRH L-mode discharges in DIII-D was shown to be consistent with the ITER89-P empirical L-mode scaling law (Luce *et al* 1991). A confinement degradation with power $\tau_E \sim P^{-0.5}$ has also been confirmed in recent experiments in TCV (Pochelon *et al* 1997) as well as the benefit of increased elongation (Fig 4) but a density dependence stronger than predicted by ITER89-P was observed (Pochelon *et al* 1998). Again a similar power degradation was observed in T-10 (Alikaev *et al* 1987) but the scaling of energy confinement time with density (plasma current) was stronger (weaker)

than predicted by ITER89-P. In RTP, improved confinement is observed at low density and plasma current but generally τ_E is somewhat less than predicted by ITER89-P (Konings *et al* 1994).

ECRH experiments in RTP, with high resolution Thomson scattering, have revealed evidence for small scale magnetic structures (Lopes Cardozo *et al* 1994). The measured electron temperature and pressure profiles exhibit several distinct features, namely hot filaments in the core, a steep gradient (up to 200keV/m) at the sawtooth inversion radius indicative of a strong transport barrier and quasi-periodic structures outside the sawtooth region (Fig 5). Measurements at ECRH turn-off indicate that the filaments have a lifetime of several hundred microseconds. Studies with off-axis ECRH (De Baar *et al* 1997) revealed the existence of transport barriers in the vicinity of other rational q surfaces besides q = 1. As a result the plasma response is extremely sensitive to the location of power deposition in the vicinity of the transport barriers and the existence of the transport barriers can lead to the appearance of a bifurcation in the confinement.

Steady-state hollow electron temperature profiles have been sustained in RTP with strong off-axis ECRH in high density plasmas creating a region of reversed magnetic shear inside which the electron thermal diffusivity is close to neoclassical (Hogeweij *et al* 1996a). At low densities ($n_{e0} < 3.5 \times 10^{19}$ m^{-3}) the temperature profile is flat inside the radius of power deposition. These results are in contrast to the so-called 'inward heat pinch' observed in DIII-D (Petty and Luce 1994) although, as in DIII-D, there was evidence for a heat flow against the temperature gradient. In the DIII-D experiments the inward energy flow returns via the ion channel and the different behaviour in RTP and DIII-D might be attributable to the different collisionality regimes in the two experiments (Hogeweij *et al* 1996b). The interpretation of such experimental data depends critically on an accurate knowledge of the electron-ion coupling which is often hindered by the relative inaccuracy of ion temperature measurements. The response to off-axis deposition in the stellarator W7-AS is also very different to that in DIII-D (Renner *et al* 1989) but preliminary experiments in TdeV do indicate the possibility of an inward heat pinch (Demers *et al* 1997). Transient shear reversal configurations have been established by heating during the current ramp up in FTU (Barbato *et al* 1997). Very high central electron temperatures, up to $T_{e0} \sim 9$keV, were obtained with only 300kW of injected power (140GHz) and very low electron thermal diffusivities ($\chi_e \sim 0.2 m^2/s$) were inferred in the plasma core. In COMPASS-D (Valovic *et al* 1997) high power heating at the end of the current ramp has been successfully employed to establish quasi-stationary single null divertor discharges with high normalised beta ($\beta_N \sim 2$). With heating later in the discharge in COMPASS-D, the achievable beta is limited by the onset of neoclassical tearing modes (Gates *et al* 1997).

ECRH has been used as a perturbative technique to study heat transport in plasmas on many devices (Erckmann and Gasparino 1994 and references therein, Deliyanakis *et al* 1994, Erckmann *et al* 1995b, Hartfuss *et al* 1994, Jacchia *et al* 1994, Peters *et al* 1995, Mantica *et al* 1996, Stroth *et al* 1996, Hogeweij *et al* 1997, Ryter *et al* 1997a, Ryter *et al* 1997b). Such studies yield incremental quantities and in principle allow diffusive and convective terms to be distinguished. Comparison with transport coefficients derived from the steady state power balance gives information on the scaling of the coefficients. Of course, in general the incremental and steady-state transport coefficients should not necessarily be equal. Although perturbative transport studies may be carried out using

sawteeth, ECRH allows the introduction of a much more controllable local temperature perturbation with a well-controlled deposition region, repetition frequency and amplitude. On the other hand, incomplete single pass absorption can lead to broadened deposition and an overestimate of the thermal diffusivity χ. In ASDEX-U, the thermal diffusivity derived from ECRH modulation (χ^{ECRH}) correlates well with power balance values (χ^{PB}) with $\chi^{ECRH} \leq 2\chi^{PB}$, whereas there is little correlation between χ^{PB} and the thermal diffusivity derived from sawteeth (χ^{ST}) as seen in Fig 6 (Ryter *et al* 1997a). The steady-state and incremental electron thermal diffusivities are generally comparable in the stellarator W7-AS (Hartfuss *et al* 1994) and the observed power degradation is not consistent with the thermal diffusivity being a function of local parameters only; in this case all data can be consistently described if χ is allowed to vary almost instantaneously in a non-local way with heating power (Stroth *et al* 1996). This model also provides a satisfactory description of RTP data but a local model can match the data equally well provided the heat flux comprises inward and outward terms (Hogeweij *et al* 1997).

Reliable access to the H-mode with ECRH has been demonstrated in many tokamaks (Lohr *et al* 1988, Hoshino *et al* 1988, Roberts *et al* 1996, Fielding *et al* 1996, Demers *et al* 1998) and in the W7-AS stellarator (Erckmann *et al* 1993). In DIII-D the power threshold for the transition from L-mode to H-mode was found to be about the same for ECRH H-modes as for NBI H-modes (Lohr *et al* 1988) and the improvement in confinement above L-mode scaling was a factor of 2 (Prater *et al* 1989). Extensive H-mode studies have been carried out in COMPASS-D at both the fundamental and second harmonic. The H-mode threshold power was found to increase sharply at low density (Fielding *et al* 1998) departing significantly from the ITER97 power threshold scaling $P_{th} \sim (n_e B_\phi)^{0.8}$ (Snipes 1997). At the highest densities the observed threshold power was close to the ITER97 predictions. Similarly in TEXT-U, the threshold power was found to exceed ITER database predictions at low density by a factor of more than x3 (Roberts *et al* 1996) and in preliminary TdeV experiments a threshold density is observed below which the H-mode cannot be achieved with the available power (Demers *et al* 1998). In both JFT-2M (Hoshino *et al* 1989) and COMPASS-D (Fielding *et al* 1998) the threshold power was reduced for off-axis heating compared with on-axis heating. An edge temperature threshold for the H-mode transition was inferred in JFT-2M (Hoshino *et al* 1988). Confinement in fundamental ECRH ELMy H-mode discharges in COMPASS-D lies somewhat below (x0.5 - 0.8) the predictions of the ITER scaling laws 0.85xITER93H and ITERH97-P (Cordey 1997) if full power absorption is assumed, whereas ohmic H-mode confinement is in good agreement with the ITER scaling laws (Fielding *et al* 1998). H-modes in the stellarator W7-AS display many of the characteristics associated with tokamak H-modes (Wagner *et al* 1994). However there were no strong isotope effects and H-modes were only observed for a very narrow operational range in rotational transform. A density threshold is observed below which H-modes are not observed with the available power.

Density 'pump-out' or 'clamping' during ECRH is commonly observed in both tokamaks and stellarators (Erckmann and Gasparino 1994 and references therein) including recent high frequency experiments in TCV (Pochelon *et al* 1998) and TdeV (Demers *et al* 1998). However this phenomenon was not observed in DIII-D or in initial FTU experiments (Cirant *et al* 1995). High power core ECRH typically leads to the generation of flat or hollow central density profiles although the overall effect on the

line-averaged density is often relatively small. The pump-out effect is still evident when ECRH is combined with NBI (Erckmann *et al* 1995a) or LHCD (Warrick *et al* 1995). As a result, ECRH has been used as an effective tool for density control in NBI-heated discharges in W7-AS (Erckmann *et al* 1995a) with no significant reduction in the global energy confinement with the addition of ECRH. Quantitative analysis is usually difficult because of uncertainties over recycling coefficients and neutral density profiles and, as a result, the underlying physical processes are still not understood. In some cases there appears to be evidence that the density behaviour is linked to pressure profile resilience (van Gelder *et al* 1998). In JFT-2M (Nagashima *et al* 1995) the measured temporal behaviour of the density perturbations produced during pulsed and modulated ECRH was well-described by numerical simulations incorporating a local ECRH-induced outward particle flux. In stellarators the loss of energetic trapped electrons is often thought to play a key role (Zushi *et al* 1994, Idei *et al* 1995) and transitions to improved particle confinement have been observed in some circumstances (Zushi *et al* 1994). There is also a clear indication in several devices of reduced impurity confinement during ECRH (Erckmann and Gasparino 1994 and references therein) which may be of great value for long pulse or cw operation in future devices. During ECRH in COMPASS-D the impurity confinement is impaired relative to that during ohmic (L-mode) plasmas by about a factor of two (Peacock *et al* 1994).

4. Electron Cyclotron Current Drive

Electron Cyclotron Current Drive (ECCD) relies on the generation of an asymmetric resistivity due to the selective heating of electrons moving in a particular toroidal direction (Fisch and Boozer 1980). Strongly upshifted or downshifted absorption, where the wave interacts with energetic electrons, is advantageous for high current drive efficiency and in the high energy limit the expected ECCD efficiency approaches that of LHCD. However, a number of physical mechanisms can limit the achievable efficiency, e.g. incomplete single pass absorption leading to counter-streaming currents on opposite sides of the resonance, transport losses (important in small devices), trapped particle effects etc. Interpretation of experimental data is also difficult in many cases leading to large uncertainties in estimates of the driven current I_{rf}. Generally $I_{rf} << I_p$ and the bootstrap current may also be significant. Estimates of the bootstrap current and the ohmically driven current must take account of non-Maxwellian electron distributions. The synergistic interaction between the ECCD and any residual dc electric field can lead to different inferred efficiencies for co- and counter- injection. Transient effects may also lead to errors unless the pulse length is comparable with the current redistribution time. In many respects the situation is simpler in stellarators (although trapping effects can be significant), which can therefore provide valuable input to the ECCD database.

Sophisticated Fokker-Planck codes have been developed in order to interpret experimental data (Westerhof 1995 and references therein). These codes have been benchmarked in several ways and good agreement is obtained with experimental data and between the different codes themselves (Westerhof 1995). Consequently the codes provide a reliable predictive capability and have been exploited extensively for studies of electron cyclotron heating and current drive in ITER (Lloyd *et al* 1994, Harvey *et al* 1997, Lloyd 1997 and references therein). However, the highest experimental current drive efficiencies achieved to date remain typically a factor x 5 - 10 below the values

predicted under optimim conditions in ITER, implying a certain degree of uncertainty in the efficiencies extrapolated to the high temperature ITER plasma conditions.

In many early ECCD experiments the inferred current drive efficiency was reported to be well below the theoretically predicted one (Erckmann and Gasparino 1994 and references therein). The influence of transport losses on the current drive efficiency was already recognised during ECCD experiments (XM, LFS, $2\omega_{ce}$) in the CLEO tokamak (Lloyd *et al* 1988). Since the Fisch-Boozer mechanism ultimately relies on momentum transfer between electrons and ions, the current drive efficiency can be significantly reduced if electron transport losses compete on a similar timescale to collisional relaxation (O'Brien *et al* 1991). Similarly in T-10 current drive experiments (OM, LFS, ω_{ce}), good agreement with theoretical modelling was obtained by taking account of the anomalous transport of the resonant electrons (Alikaev *et al* 1992b). Nevertheless, in this case, fully non-inductively driven discharges were obtained at low plasma current where the contribution of the bootstrap current was significant (> 50%). The sustainment of a pre-existing fast electron tail by ECCD with zero loop voltage was shown at WT-2 for first harmonic (Ando *et al* 1986) and WT-3 for second harmonic downshifted heating (Tanaka *et al* 1991) in very low density plasmas.

Recent current drive experiments in T-10 have been reviewed by Esipchuk 1995 (see also Alikaev *et al* 1995, Razumova *et al* 1995). Current drive efficiencies up to $\eta_{20} = n_e\,(x10^{20}m^{-3})\,R_oI_{rf}/P_{rf} = 0.013\ AW^{-1}m^{-2}$ were obtained at the second harmonic (140GHz, XM, LFS) and up to $0.033\ AW^{-1}m^{-2}$ at the first harmonic (81.3GHz, OM, LFS). The experimental results were generally in qualitative agreement with Fokker-Planck calculations but interpretation in some cases was complicated by the different sawtooth behaviour with co- and counter-injection and there was also evidence to suggest that non-linear processes might be important. Transport losses and the non-optimum launch polarisation were also considered in the analysis.

The effect of the residual dc electric field was confirmed in COMPASS-D (Todd *et al* 1993) and DIII-D (James *et al* 1995, Petty *et al* 1995) 60GHz ECCD experiments. In both cases the data were well-described by Fokker-Planck calculations which included trapping and the effects of the dc electric field. Current drive efficiencies up to $\eta_{20} \sim 0.015\ AW^{-1}m^{-2}$ were achieved with downshifted absorption in DIII-D (including synergistic effects) and complete non-inductive current drive was obtained with ECCD + FWCD (fast wave current drive) at low plasma current (~ 170kA). Detailed kinetic and current profile measurements are available in DIII-D, allowing the non-inductive current profile to be evaluated (Forest *et al* 1994) and avoiding the need for co/counter comparisons to evaluate the current drive efficiency. Preliminary 110GHz experiments (LFS, $2\omega_{ce}$) indicate a driven current of ~ 170kA with corresponding efficiency $\eta_{20} \sim 0.035$ - $0.04\ AW^{-1}m^{-2}$ (Luce *et al* 1997). Experiments in COMPASS-D have demonstrated that the beta limit is extended (Fig 7), and confinement is improved, in discharges with counter-ECCD in the core versus those with co-current drive (Gates *et al* 1995). The ECCD contribution could be adjusted using toroidally steerable antennas. The loop voltage was very close to zero in these high beta discharges but the contribution of the bootstrap current is dominant, the plasma conductivity is very high ($\langle T_e \rangle \sim 5$keV) and the ECCD efficiency is therefore difficult to estimate reliably.

In RTP, similar current drive efficiencies $\eta_{20} \sim 0.005$ $AW^{-1}m^{-2}$ were inferred for fundamental (60GHz) and second harmonic (110GHz) current drive (Polman *et al* 1997a, Polman *et al* 1997b). The driven currents were in qualitative agreement with Fokker-Planck calculations but the role of non-linear effects remains uncertain. Preliminary second harmonic ECCD experiments in TCV (Goodman *et al* 1998) are also in agreement with theoretical predictions.

Extensive ECCD experiments have been carried out in W7-AS, at 70GHz and 140GHz, and many of the results are described in the review by Erckmann and Gasparino 1994. Various scenarios have been investigated including those in which the driven current is compensated by an inductively driven current and those in which the driven current is allowed to freely develop. ECCD has also been used to compensate the bootstrap current. Excellent agreement with theory is generally obtained when the effects of trapping in the complex 3D stellarator geometry are included. The role of trapping was investigated by conducting experiments in various magnetic configurations (Erckmann *et al* 1995a). Perturbation experiments (140GHz, XM) with oppositely directed (toroidally) ECRH beams, modulated in-phase or out of phase, allowed the ECCD and bootstrap current contributions to be discriminated (Erckmann *et al* 1995b). ECCD has also been used to investigate the influence of local shear modification on confinement (Erckmann *et al* 1997).

5. Instability Control

The localised nature of the electron cyclotron wave-plasma interaction has been used to good effect for the control of various instabilities. Sawtooth suppression by local heating in the vicinity of $q = 1$ has been demonstrated in many experiments (Erckmann and Gasparino 1994 and references therein, Pochelon *et al* 1998) with powers of the order of or greater than the ohmic power P_{OH}, whereas central heating tends to be destabilising. The experimental results are qualitatively consistent with a local flattening of the current and/or pressure profiles in the vicinity of the resonant surface. Second harmonic electron cyclotron current drive has recently been employed for sawtooth stabilisation in T-10 (Kislov *et al* 1995). Sawteeth were stabilised both with on-axis counter-ECCD and off-axis co-ECCD at a power level of ~ 0.5MW.

The control of low-order internal MHD modes, particularly the m=2, n=1 tearing mode is important for optimising plasma performance and avoiding disruptions. The plasma stability may be influenced by shaping of the equilibrium current profile in the vicinity of the resonant surface or by modification of the local current density inside the island which may be optimised by modulation of the injected power in phase with the rotating island. Modulated ECCD is predicted to be more efficient than steady-state ECCD or modulated ECRH. Second harmonic ECRH (157GHz, perpendicular launch) and ECCD (140GHz, oblique launch) stabilisation experiments have recently been carried out in T-10 (Kislov *et al* 1997). In low q discharges the m=2, n=1 tearing mode was partially suppressed by heating (157GHz) in the vicinity of q=2 (Fig 8). The effect increases with absorbed ECRH power. For an absorbed power equal to 15% of the total input power the island width was reduced by 35%. The suppression was attributed to a reduction of the resistivity in the island O-pt rather than an axisymmetric current density redistribution. Power deposition near the X-pt cannot produce the same local perturbation because of the magnetic field line configuration, thus preventing an

equivalent destabilising effect. Therefore joint heating of the island O- and X-pts, as takes place in the case of a rotating island, is still expected to produce a favourable stabilising effect. The effect of current drive was studied at 140GHz. Although partial suppression was observed, there was no difference between co- and counter- current drive because of the insufficient values of driven current produced under the operating conditions of the experiment. In experiments near the density limit, ECRH was effective in extending the operational density range by ~ 15% (Fig 8) practically independently of the resonance location, indicating perhaps the influence of improved global energy balance, although the stabilising effect on m=2 activity was increased for resonance near q=2. In earlier T-10 experiments (Savrukhin *et al* 1994) it was observed that density limit disruptions in plasmas with high edge q were often associated with coupling of m=2, n=1 and m = 1, n = 1 modes which overlap at the energy quench stage. Second harmonic ECRH was used to suppress the m=2 activity preventing mode overlap and allowing stable operation up to higher density. Mode suppression was observed with both on- and off-axis ECRH but complete stabilisation of the m=2 activity was achieved with lower power when the ECRH was resonant just outside q=2. ECRH switched on *during* the disruption allowed stable operation to be recovered after the energy quench. Similar results on ECRH control of the current quench have recently been reported in RTP (Salzedas *et al* 1998). Avoidance of radiative disruptions by core ECRH has been reported in MTX (Rice and Hooper 1994). In WT-3 (Terumichi *et al* 1995) the m=2, n=1 tearing mode was suppressed by second harmonic heating at q=1 and sawteeth were modified by ECRH resonant at q=2. In each case the heating had to be narrowly localised near the rational surface. Suppression was very fast, much shorter than the current diffusion time, indicating the role of mode coupling. In JFT-2M, q=3 disruptions could be avoided when second harmonic ECRH in the vicinity of the q=2 rational surface was used to suppress m=2 activity (Hoshino *et al* 1995). As in the case of T-10 low q experiments, the stabilising effect was attributed to direct island heating. Mode locking and disruption at the density limit could also be avoided by ECRH, with power levels greater than ~ 20% P_{OH}, leading to an increase in the operating density range of 10 - 15%. In contrast to T-10, there was no improvement unless the ECRH resonance was located close to q=2.

Feedback pulse modulation of the ECRH power, resonant at the q=2 surface and synchronised to the rotating 2,1 island, was also successfully employed in JFT-2M (Hoshino *et al* 1995). O-pt heating was effective in partially suppressing the 2,1 tearing mode whereas X-pt heating had no effect (Fig 9). However, the effectiveness of the modulated O-pt heating was only comparable with that achievable with unmodulated ECRH. Similar experiments were carried out in COMPASS-D (McArdle *et al* 1995) where the feedback system could track rapid changes in mode frequency while maintaining a constant programmable phase relationship between the ECRH pulse and the rotating 2,1, island. Effective stabilisation was observed for power deposited close to q=2 in both modulated and unmodulated cases. Although there were some indications of phase sensitive effects, the results were inconclusive regarding the benefits of modulation.

Second harmonic heating resonant close to q=2 was also used in COMPASS-D to remove or prevent error-field driven locked modes (Morris *et al* 1995). The results were insensitive to the relative toroidal phase relationship between the locked mode and the ECRH antennas (i.e. X-pt versus O-pt heating). Suppression of locked modes in low

density and low q discharges has been demonstrated with central ECRH in T-10 (Ivanov *et al* 1995) for power levels > 0.5MW. In WT-3 (Maekawa *et al* 1997), second harmonic ECRH was effective in preventing LHCD-induced mode locking thereby avoiding disruption. The results were not sensitive to the resonance location in this case.

ELM control using ECRH has been demonstrated in DIII-D (Luxon *et al* 1990) and COMPASS-D (Morris *et al* 1995). In DIII-D the ELM frequency was increased or decreased depending on whether the power was deposited inside or outside the separatrix. In COMPASS-D, ECRH just inside the separatrix resulted in a decrease in ELM frequency for a wide range of conditions (or triggered a transition to ELM-free H-mode) which may simply reflect the commonly observed frequency variation of Type-III ELMs with power (moving the resonance towards the plasma core delayed the frequency change).

6. Preionisation and Start-up

ECRH has been used effectively for preionisation and startup-assist in many tokamaks and is used routinely for plasma production in stellarators (Lloyd *et al* 1991, Erckmann and Gasparino 1994 and references therein; Yao *et al* 1994, Zhang *et al* 1995, Abrakov *et al* 1997). In tokamaks the confinement is poor during start-up, which as a consequence is very sensitive to stray magnetic fields, whereas in stellarators the external coils provide magnetic confinement during breakdown. In early tokamak experiments, ECRH preionisation typically led to a reduction of x 2 - 5 in the initial loop voltage together with a smaller reduction in the overall flux consumption during the current rise phase. Features common to many of these early experiments include an insensitivity to the wave launching scenario (i.e. inboard/outboard launch, XM/OM polarisation), effective preionisation at the second harmonic and a weak dependence on the resonance location. The effective use of the OM for preionisation has been attributed to the depolarising effect of wall reflections and this scheme will be exploited in ITER (Lloyd *et al* 1996). In small devices the upper hybrid resonance (UHR) plays a key role during start-up (Whaley *et al* 1992, Polman *et al* 1992). After initial breakdown at the cyclotron resonance layer the dominant interaction becomes linear mode conversion of the XM to the electron Bernstein wave (EBW) at the UHR. The EBW is strongly absorbed in the region between the UHR and the cyclotron resonance layer. In larger devices, absorption at the cyclotron resonance layer becomes the dominant mechanism. Various detailed theoretical descriptions of ECRH preionisation in tokamaks have been developed (Maroli and Petrillo 1988, Pereverzev 1989, Fidone and Granata 1994).

In ITER, where the applied electric field is limited to ~ 0.3V/m, ECRH may be necessary to provide robust and reliable start-up. A systematic series of experiments was carried out on DIII-D in order to study low voltage start-up with and without ECRH to provide data which could be readily extrapolated to ITER (Lloyd *et al* 1991). It was shown that for low voltage start-up ECRH not only leads to improved start-up reliability, but permits operation over a greatly extended range of prefill pressure and stray magnetic field and leads to reduced runaway generation. Prompt ECRH-assisted start-up with an electric field of ~ 0.15V/m was demonstrated. For ECRH-assisted start-up in ITER, the power and pulse length requirements will be essentially determined by the need to ensure burnthrough, i.e. complete ionisation of hydrogen and the transition to high ionisation states of impurities. Detailed modelling of the burnthrough phase in

ITER (Lloyd *et al* 1996) has indicated that an *absorbed* ECRH power of ~ 3MW will ensure reasonably robust start-up for a broad range of conditions with up to 5% beryllium impurity.

7. Summary and Conclusions

Effective heating and current drive using electron cyclotron waves has been demonstrated in many devices. The physics of wave propagation and absorption is well-understood and detailed aspects of the theory have been confirmed in the latest generation of high frequency experiments with good beam focusing and steerability. Present experiments are well-described by sophisticated Fokker-Planck codes which provide a reasonably reliable predictive capability for future devices. Nevertheless, the highest current drive efficiencies achieved so far are a factor x 5 - 10 below those expected in ITER because of the relatively low temperatures in present devices. The localised and controllable nature of the wave-particle interaction has been extensively exploited for perturbative transport studies and for the control of various instabilities. Furthermore, ECRH has been used effectively for preionisation and start-up assist in many devices. The latest generation of experiments further confirm that ECRH is a highly efficient, controllable and flexible auxiliary heating and current drive system with the potential to fulfil many functions in Next Step devices.

Acknowledgements
This work was jointly funded by the UK Department of Trade and Industry and Euratom. The author is extremely grateful for the material provided by the many contributors to this review.

References

Abrakov V V *et al* 1997 *Nucl. Fusion* **37** 233.

Alikaev V V *et al* 1987 *Sov. Journal Plasma Phys.* **13** 1.

Alikaev V V *et al* 1992a *High-Frequency Plasma Heating* (New York: American Institute of Physics).

Alikaev V V *et al* 1992b *Nucl. Fusion* **32** 1811.

Alikaev V V *et al* 1995 *Nucl. Fusion* **35** 369.

Allen S L *et al* 1994 *Phys. Rev. Lett.* **72** 1348.

Ando A *et al* 1986 *Phys. Rev. Lett.* **56** 2180.

Barbato E *et al* 1997 *Proc. 24th European Conf. on Controlled Fusion and Plasma Physics (Berchtesgaden, 1997)* vol 21A part III (Lausanne: European Physical Society) p 1161.

Batchelor D B and Bigelow T S 1997 *AIP Conf. Proc. 403, Radio Frequency Power in Plasmas (Savannah)* ed P M Ryan and T Intrator p 215.

Bornatici M *et al* 1983 *Nucl. Fusion* **23** 1153.

Boyd D *et al* 1995 *Proc. 9th Joint Workshop on ECE and ECRH* (Borrego Springs, USA) p 255.

Buratti P *et al* 1995 *Proc. 22nd European Conf. on Controlled Fusion and Plasma Physics (Bournemouth, 1995)* vol 19C part III (Lausanne: European Physical Society) p 21.

Chan V S *et al* 1997 *Proc. 16th Int. Conf. on Plasma Physics and Controlled Nuclear Fusion Research (Montreal, 1996)* vol I (Vienna: IAEA) p 95.

Cirant S *et al* 1995 *Proc. 15th Int. Conf. on Plasma Physics and Controlled Nuclear Fusion Research (Seville, 1994)* vol II (Vienna: IAEA) p 159.

Cirant S *et al* 1996 *Proc. 23rd European Conf. on Controlled Fusion and Plasma Physics (Kiev, 1996)* vol 20C part II (Lausanne: European Physical Society) p 883.

Cordey J G 1997 *Plasma Phys. Control. Fusion* **39** B115.

De Baar M R *et al* 1997 *Phys. Rev. Lett.* **78** 4573.

Deliyanakis N *et al* 1994 *Plasma Phys. Control. Fusion* **36** 1391.

Demers Y *et al* 1997 *Bull. Am. Phys. Soc.* **42** 1856.

Demers Y *et al* 1998 *2nd Europhysics Top. Conf. on Radiofrequency Heating and Current Drive of Fusion Devices, Europhysics Conf. Abstracts (Brussels, Belgium)* vol 22A p 281.

Erckmann V V *et al* 1993 *Phys. Rev. Lett.* **70** 2086.

Erckmann V and Gasparino U 1994 *Plasma Phys. Control. Fusion* **36** 1869.

Erckmann V *et al* 1995a *Fusion Engineering and Design* **26** 141.

Erckmann V *et al* 1995b *Proc. 15th Int. Conf. on Plasma Physics and Controlled Nuclear Fusion Research (Seville, 1994)* vol I (Vienna: IAEA) p 771.

Erckmann V *et al* 1997 *Proc. 16th Int. Conf. on Plasma Physics and Controlled Nuclear Fusion Research (Montreal, 1996)* vol II (Vienna: IAEA) p 119.

Esipchuk Yu V 1995 *Plasma Phys. Control. Fusion* **37** A267.

Fidone I and granata G 1994 *Nucl. Fusion* **34** 743.

Fielding S J *et al* 1996 *Plasma Phys. Control. Fusion* **38** 1091.

Fielding S J *et al* 1998 *Plasma Phys. Control. Fusion* **40** 731.

Fisch N J and Boozer A H 1980 *Phys. Rev. Lett.* **45** 720.

Forest C B *et al* 1994 *Phys. Rev. Lett.* **73** 2444.

Gates D A *et al* 1995 *Proc. 22nd European Conf. on Controlled Fusion and Plasma Physics (Bournemouth, 1995)* vol 19C part IV (Lausanne: European Physical Society) p 117.
Gates D A *et al* 1997 *Proc. 16th Int. Conf. on Plasma Physics and Controlled Nuclear Fusion Research (Montreal, 1996)* vol I (Vienna: IAEA) p 715.
Giruzzi G *et al* 1995 *Proc. 9th Joint Workshop on ECE and ECRH* (Borrego Springs, USA) p 247.
Goodman T P *et al* 1998 *2nd Europhysics Top. Conf. on Radiofrequency Heating and Current Drive of Fusion Devices, Europhysics Conf. Abstracts (Brussels, Belgium)* vol 22A p 245.
Hartfuss H J *et al* 1994 *Plasma Phys. Control. Fusion* **36** B17.
Harvey R W *et al* 1997 *Nucl. Fusion* **37** 69.
Hogeweij G M D *et al* 1996a *Phys. Rev. Lett.* **76** 632.
Hogeweij G M D *et al* 1996b *Nucl. Fusion* **36** 535.
Hogeweij G M D *et al* 1997 *Proc. 16th Int. Conf. on Plasma Physics and Controlled Nuclear Fusion Research (Montreal, 1996)* vol I (Vienna: IAEA) p 655.
Hoshino K *et al* 1988 *Nucl. Fusion* **28** 301.
Hoshino K *et al* 1989 *Phys. Rev. Lett.* **63** 770.
Hoshino K *et al* 1995 *Proc. 15th Int. Conf. on Plasma Physics and Controlled Nuclear Fusion Research (Seville, 1994)* vol I (Vienna: IAEA) p 697.
Idei H *et al* 1995 *Fusion Engineering and Design* **26** 167.
Ivanov N V *et al* 1995 *Proc. 22nd European Conf. on Controlled Fusion and Plasma Physics (Bournemouth, 1995)* vol 19C part III (Lausanne: European Physical Society) p 77.
Jacchia A *et al* 1994 *Nucl. Fusion* **34** 1629.
James R *et al* 1995 *Proc. 9th Joint Workshop on ECE and ECRH* (Borrego Springs, USA) p 75.
Jotaki E and Itoh S 1997 *Kyushu University Report* FURKU 97-03(44).
Kawashima H *et al* 1991 *Nucl. Fusion* **31** 495.
Kislov D A *et al* 1995 *Proc. 22nd European Conf. on Controlled Fusion and Plasma Physics (Bournemouth, 1995)* vol 19C part I (Lausanne: European Physical Society) p 369.
Kislov D A *et al* 1997 *Nucl. Fusion* **37** 339.
Konings J A *et al* 1994 *Plasma Phys. Control. Fusion* **36** 45.
Laqua H P *et al* 1997 *Phys. Rev. Lett.* **78** 3467.
Leuterer F *et al* 1997 *Proc. 24th European Conf. on Controlled Fusion and Plasma Physics (Berchtesgaden, 1997)* vol 21A part IV (Lausanne: European Physical Society) p 1533.
Lohr J *et al* 1988 *Phys. Rev. Lett.* **60** 2630.
Lloyd B *et al* 1988 *Nucl. Fusion* **28** 1013.
Lloyd B *et al* 1991 *Nucl. Fusion* **31** 2031.
Lloyd B *et al* 1994 *Proc. 21st European Conf. on Controlled Fusion and Plasma Physics (Montpellier, 1994)* vol 18B part II (Lausanne: European Physical Society) p 1012.
Lloyd B *et al* 1996 *Plasma Phys. Control Fusion* **38** 1627.
Lloyd B 1997 *Proc. 10th Joint Workshop on ECE and ECRH* (Ameland, Holland) p 443.
Lopes Cardozo N J *et al* 1994 *Phys. Rev. Lett.* **73** 256.

Luce T C *et al* 1991 *Proc. 13th Int. Conf. on Plasma Physics and Controlled Nuclear Fusion Research (Washington, 1990)* vol I (Vienna: IAEA) p 631.
Luce T C *et al* 1997 *Bull. Am. Phys. Soc.* **42** 1976.
Luxon J L *et al* 1990 *Plasma Phys. Control. Fusion* **32** 869.
Maekawa T *et al* 1997 *Proc. 16th Int. Conf. on Plasma Physics and Controlled Nuclear Fusion Research (Montreal, 1996)* vol I (Vienna: IAEA) p 771.
Mantica P *et al* 1996 *Nucl. Fusion* **36** 1317.
Maroli C and Petrillo V 1988 *Nuovo Cimento* D **10** 677.
McArdle G J *et al* 1995 *Proc. 9th Joint Workshop on ECE and ECRH* (Borrego Springs, USA) p 271.
Michelot Y *et al* 1996 *Nucl. Fusion* **36** 309.
Morris A W *et al* 1995 *Proc. 15th Int. Conf. on Plasma Physics and Controlled Nuclear Fusion Research (Seville, 1994)* vol I (Vienna: IAEA) p 365.
Nagashima K *et al* 1995 *Nucl. Fusion* **35** 994.
O'Brien M R *et al* 1991 *Nucl. Fusion* **31** 583.
Peacock N J *et al* 1994 *Proc. 21st European Conf. on Controlled Fusion and Plasma Physics (Montpellier, 1994)* vol 18B part I (Lausanne: European Physical Society) p 134.
Peeters A G *et al* 1995 *Plasma Phys. Control. Fusion* **37** 525.
Peters M *et al* 1995 *Proc. 22nd European Conf. on Controlled Fusion and Plasma Physics (Bournemouth, 1995)* vol 19C part III (Lausanne: European Physical Society) p 37.
Pereverzev G V 1989 *Proc. 12th Int. Conf. on Plasma Physics and Controlled Nuclear Fusion Research (Nice, 1988)* vol I (Vienna: IAEA) p 739.
Petty C C *et al* 1995 *Nucl. Fusion* **35** 773.
Petty C C and Luce T C 1994 *Nucl. Fusion* **34** 121.
Pochelon A *et al* 1997 *Proc. 24th European Conf. on Controlled Fusion and Plasma Physics (Berchtesgaden, 1997)* vol 21A part II (Lausanne: European Physical Society) p 537.
Pochelon A *et al* 1998 *2nd Europhysics Top. Conf. on Radiofrequency Heating and Current Drive of Fusion Devices, Europhysics Conf. Abstracts (Brussels, Belgium)* vol 22A p 253.
Polman R W *et al* 1992 *Europhysics Top. Conf. on Radiofrequency Heating and Current Drive of Fusion Devices, Europhysics Conf. Abstracts (Brussels, Belgium)* vol 16E p 321.
Polman R W *et al* 1997a *Proc. 24th European Conf. on Controlled Fusion and Plasma Physics (Berchtesgaden, 1997)* vol 21A part II (Lausanne: European Physical Society) p 605.
Polman R W *et al* 1997b *Proc. 10th Joint Workshop on ECE and ECRH* (Ameland, Holland) p 357.
Prater R *et al* 1989 *Proc. 12th Int. Conf. on Plasma Physics and Controlled Nuclear Fusion Research (Nice, 1988)* vol I (Vienna: IAEA) p 527.
Prater R 1990 *Journal of Fusion Energy* **9** 19.
Preinhaelter J and Kopecky V 1973 J. Plasma Physics **10** 1.
Razumova K A *et al* 1994 *Physics of Plasmas* **1** 1554.
Renner H *et al* 1989 *Plasma Phys. Control. Fusion* **31** 1579.
Rice B W and Hooper E B 1994 *Nucl. Fusion* **34** 1.
Roberts D 1995 *Proc. 9th Joint Workshop on ECE and ECRH* (Borrego Springs, USA) p 125.

Roberts D R *et al* 1996 *Plasma Phys. Control. Fusion* **38** 1117.
Rome M *et al* 1997 *Plasma Phys. Control Fusion* **39** 117.
Ryter F *et al* 1997a *Proc. 16th Int. Conf. on Plasma Physics and Controlled Nuclear Fusion Research (Montreal, 1996)* vol I (Vienna: IAEA) p 1625.
Ryter F *et al* 1997b *Proc. 24th European Conf. on Controlled Fusion and Plasma Physics (Berchtesgaden, 1997)* vol 21A part IV (Lausanne: European Physical Society) p 1477.
Salzedas F *et al* 1998 *2nd Europhysics Top. Conf. on Radiofrequency Heating and Current Drive of Fusion Devices, Europhysics Conf. Abstracts (Brussels, Belgium)* vol 22A p 273.
Savrukhin P V *et al* 1994 *Nucl. Fusion* **34** 317.
Segui J L and Giruzzi G 1994 *Plasma Phys. Control. Fusion* **36** 897.
Segui J L *et al* 1995 *Proc. 9th Joint Workshop on ECE and ECRH* (Borrego Springs, USA) p 223.
Segui J L *et al* 1996 *Nucl. Fusion* **36** 237.
Smits F M A *et al* 1992 *Europhysics Top. Conf. on Radiofrequency Heating and Current Drive of Fusion Devices, Europhysics Conf. Abstracts (Brussels, Belgium)* vol 16E p 313.
Snipes J A 1997 *Proc. 24th European Conf. on Controlled Fusion and Plasma Physics (Berchtesgaden, 1997)* vol 21A part III (Lausanne: European Physical Society) p 961.
Stroth U *et al* 1996 *Plasma Phys. Control. Fusion* **38** 611.
Tanaka H *et al* 1991 *Nucl. Fusion* **31** 1673.
Tanaka S *et al* 1992 *Europhysics Top. Conf. on Radiofrequency Heating and Current Drive of Fusion Devices, Europhysics Conf. Abstracts (Brussels, Belgium)* vol 16E p 265.
Terumichi Y *et al* 1995 *Proc. 15th Int. Conf. on Plasma Physics and Controlled Nuclear Fusion Research (Seville, 1994)* vol II (Vienna: IAEA) p 189.
Todd T N *et al* 1993 *Plasma Phys. Control Fusion* **35** B231.
Tran M Q 1998 *Plasma Phys. Control. Fusion*, to be published.
Valovic M *et al* 1997 *Proc. 24th European Conf. on Controlled Fusion and Plasma Physics (Berchtesgaden, 1997)* vol 21A part I (Lausanne: European Physical Society) p 269.
van Gelder J F M *et al* 1995 *Proc. 9th Joint Workshop on ECE and ECRH* (Borrego Springs, USA) p 239.
van Gelder J F M *et al* 1997 *Proc. 10th Joint Workshop on ECE and ECRH* (Ameland, Holland) p 185.
van Gelder J F M *et al* 1998 submitted to *Plasma Phys. Control. Fusion.*
Wagner F *et al* 1994 *Plasma Phys. Control. Fusion* **36** A61.
Warrick C D *et al* 1995 *Proc. 22nd European Conf. on Controlled Fusion and Plasma Physics (Bournemouth, 1995)* vol 19C part III (Lausanne: European Physical Society) p 369.
Westerhof E 1995 *Proc. 9th Joint Workshop on ECE and ECRH* (Borrego Springs, USA) p 3.
Whaley D R *et al* 1992 *Nucl. Fusion* **32** 757.
Yao L H *et al* 1994 *Proc. 21st European Conf. on Controlled Fusion and Plasma Physics (Montpellier, 1994)* vol 18B part II (Lausanne: European Physical Society) p 1016.

Zhang D *et al* 1995 *Proc. 9th Joint Workshop on ECE and ECRH* (Borrego Springs, USA) p 117.
Zushi H *et al* 1994 *Plasma Phys. Control. Fusion* **36** A231.

Figure Captions

Fig 1 Electron temperature evolution during a sawtoothing discharge with ECRH (140GHz) starting at 700.75ms in FTU (Cirant et al 1995).

Fig 2 Heating by O-X-B conversion in the stellarator W7-AS (Laqua et al 1997).
(a) Calculated ray trajectory and relative beam power for resonant heating (the z co-ordinate lies along the magnetic field direction) showing successive conversion of the launched ordinary wave (O-mode) to the extra-ordinary wave (X-mode) and then to the electron Bernstein wave (B-mode) which is strongly damped.
(b) Increase of plasma energy content versus the longitudinal vacuum refractive index N_z (related directly to launch angle) of the incident ordinary wave for non-resonant heating. The solid line is the transmission function (OM→XM conversion efficiency) multiplied by the maximum energy increase.

Fig 3 Electron temperature profile during initial 110GHz experiments in DIII-D (Chan et al 1997).

Fig 4 Scaling of the electron energy confinement time with power (a) and density (b) during ECRH (82.7GHz) in TCV (Pochelon et al 1998). The power scaling is shown for $q = 5$ and two different densities (2×10^{19} m^{-3} and 3×10^{19} m^{-3}). The density scaling is shown for two different elongations ($\kappa = 1.16$ and $\kappa = 1.32$).

Fig 5 Temperature profiles during ECRH in RTP (60GHz) showing filamentation in the core and strong temperature gradients near the sawtooth inversion radius. Case (c) is an averaged profile of 15 discharges with identical conditions (Lopes Cardozo et al 1994).

Fig 6 Electron thermal diffusivities derived from sawtooth and ECRH heat pulse studies (χ^{HP}) and steady state power balance (χ^{PB}) for ohmic and L-mode discharges in ASDEX-U (Ryter et al 1997a).

Fig 7 (a) Maximum poloidal beta (β_p) and normalised beta (β_N) versus toroidal launch angle (with respect to the major radius) and (b) H-factor ($\tau_E/\tau_{ITER89P}$) versus toroidal launch angle during high power second harmonic ECRH/ECCD (60GHz) in COMPASS-D (Gates et al 1995).

Fig 8 Mode suppression and extension of the density limit in T-10 (Kislov et al 1997).
(a) Amplitude of $m = 2$ perturbation versus toroidal magnetic field and thus ECRH resonance position ($q = 2.7$, $P_{ECRH} = 0.2$MW, 157GHz); (b) Maximum line-averaged density versus ECRH resonance position ($q = 4$, $P_{ECRH} = 0.2$MW, 157GHz).

Fig 9 Suppression of the $m = 2$, $n = 1$ mode in JFT-2M by O-point heating using modulated ECRH. The change in mode amplitude is plotted versus the phase relationship between the rotating mode and the modulated ECRH pulse (Hoshino et al 1995).

Figure Captions

Fig 1 Electron temperature evolution during a sawtoothing discharge with ECRH (140GHz) starting at 700.75ms in FTU (Cirant et al 1995).

Fig 2 Heating by O-X-B conversion in the stellarator W7-AS (Laqua et al 1997).
(a) Calculated ray trajectory and relative beam power for resonant heating (the z co-ordinate lies along the magnetic field direction) showing successive conversion of the launched ordinary wave (O-mode) to the extra-ordinary wave (X-mode) and then to the electron Bernstein wave (B-mode) which is strongly damped.
(b) Increase of plasma energy content versus the longitudinal vacuum refractive index N_z (related directly to launch angle) of the incident ordinary wave for non-resonant heating. The solid line is the transmission function (OM→XM conversion efficiency) multiplied by the maximum energy increase.

Fig 3 Electron temperature profile ($n_e = 0.5 \times 10^{19}$ m^{-3}) during initial 110GHz experiments in DIII-D (Chan et al 1997).

Fig 4 Scaling of the electron energy confinement time with power (a) and density (b) during ECRH (82.7GHz) in TCV (Pochelon et al 1998). The power scaling is shown for $q = 5$ and two different densities (2×10^{19} m^{-3} and 3×10^{19} m^{-3}). The density scaling is shown for two different elongations ($\kappa = 1.16$ and $\kappa = 1.32$).

Fig 5 Temperature profiles during ECRH in RTP (60GHz) showing filamentation in the core and strong temperature gradients near the sawtooth inversion radius. Case (c) is an averaged profile of 15 discharges with identical conditions (Lopes Cardozo et al 1994).

Fig 6 Electron thermal diffusivities derived from sawtooth and ECRH heat pulse studies (χ^{HP}) and steady state power balance (χ^{PB}) for ohmic and L-mode discharges in ASDEX-U (Ryter et al 1997a).

Fig 7 (a) Maximum poloidal beta (β_p) and normalised beta (β_N) versus toroidal launch angle (with respect to the major radius) and (b) H-factor ($\tau_E/\tau_{ITER89P}$) versus toroidal launch angle during high power second harmonic ECRH/ECCD (60GHz) in COMPASS-D (Gates et al 1995).

Fig 8 Mode suppression and extension of the density limit in T-10 (Kislov et al 1997).
(a) Amplitude of $m = 2$ perturbation versus toroidal magnetic field and thus ECRH resonance position ($q = 2.7$, $P_{ECRH} = 0.2$MW, 157GHz); (b) Maximum line-averaged density versus ECRH resonance position ($q = 4$, $P_{ECRH} = 0.2$MW, 157GHz).

Fig 9 Suppression of the $m = 2$, $n = 1$ mode in JFT-2M by O-point heating using modulated ECRH. The change in mode amplitude is plotted versus the phase relationship between the rotating mode and the modulated ECRH pulse (Hoshino et al 1995).

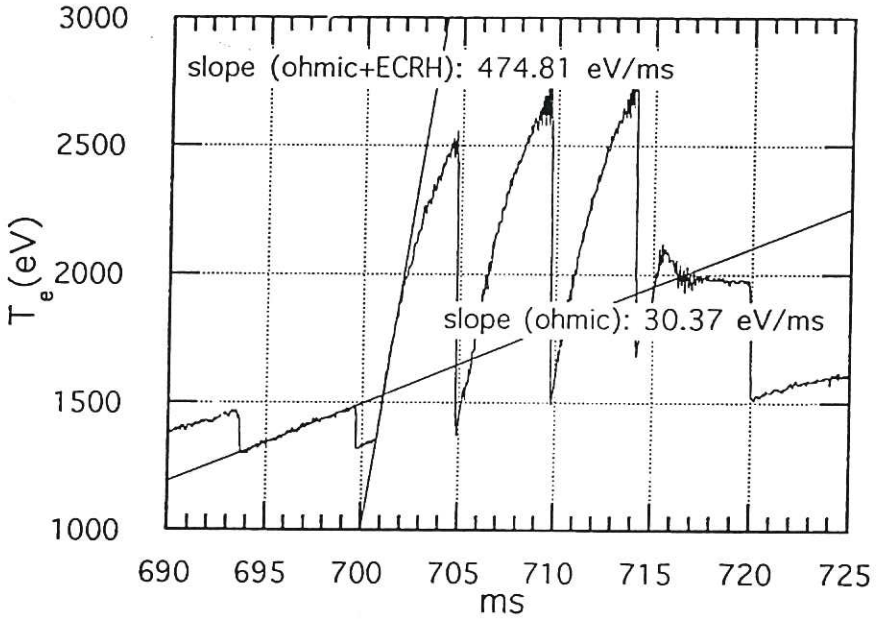
slope (ohmic+ECRH): 474.81 eV/ms
slope (ohmic): 30.37 eV/ms
T_e (eV)
3000
2500
2000
1500
1000
690
695
700
705
710
715
720
725
ms

Fig 1

(a)

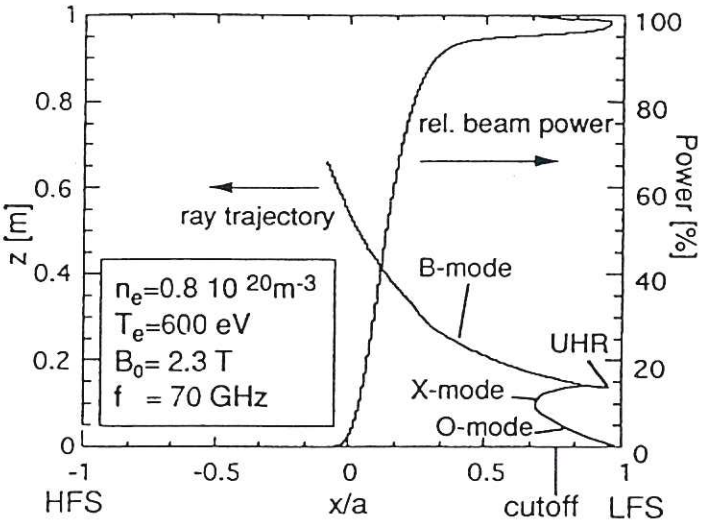
rel. beam power
ray trajectory
B-mode
UHR
X-mode
O-mode
n_e=0.8 10 ^{20}m^{-3}
T_e=600 eV
B_0= 2.3 T
f = 70 GHz
z [m]
Power [%]
HFS
x/a
cutoff
LFS

(b)

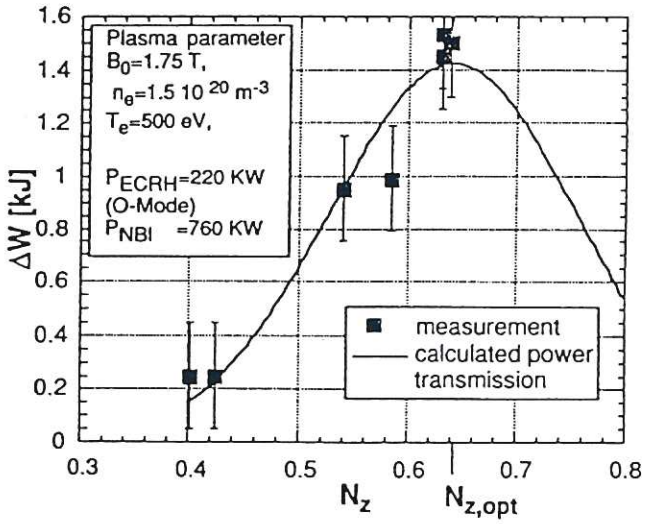
Plasma parameter
B_0=1.75 T,
n_e=1.5 10 ^{20} m^{-3}
T_e=500 eV,
P_{ECRH}=220 KW
(O-Mode)
P_{NBI} =760 KW
measurement
calculated power transmission
ΔW [kJ]
N_z
$N_{z,opt}$

Fig 2

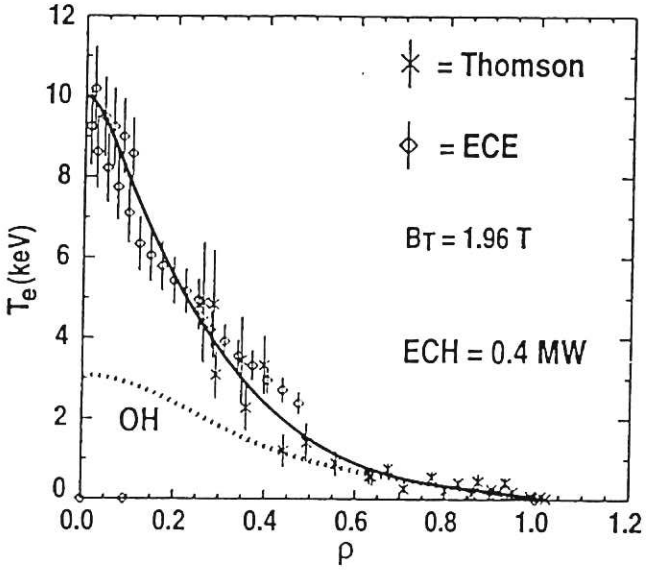
12
10
8
6
4
2
0
T_e(keV)
0.0
0.2
0.4
0.6
0.8
1.0
1.2
ρ
= Thomson
= ECE
B_T = 1.96 T
ECH = 0.4 MW
OH

Fig 3

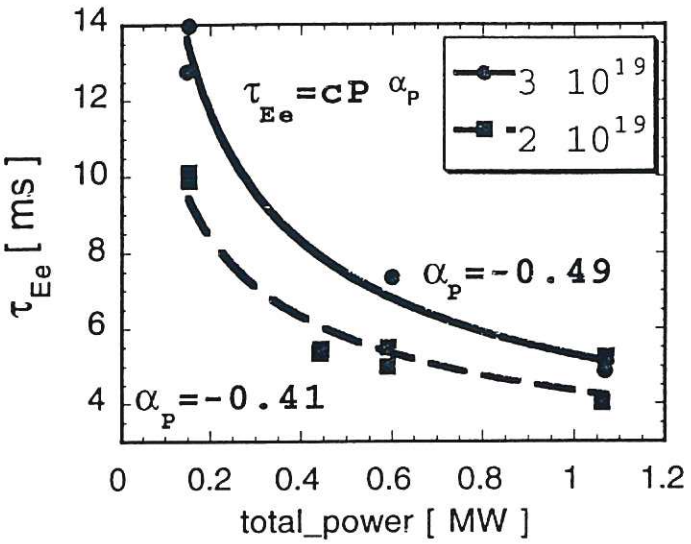
14
12
10
8
6
4
τ_{Ee} [ms]
τ_{Ee} = cP α_P
3 10^{19}
2 10^{19}
α_p = -0.49
α_p = -0.41
0
0.2
0.4
0.6
0.8
1
1.2
total_power [MW]

(a)

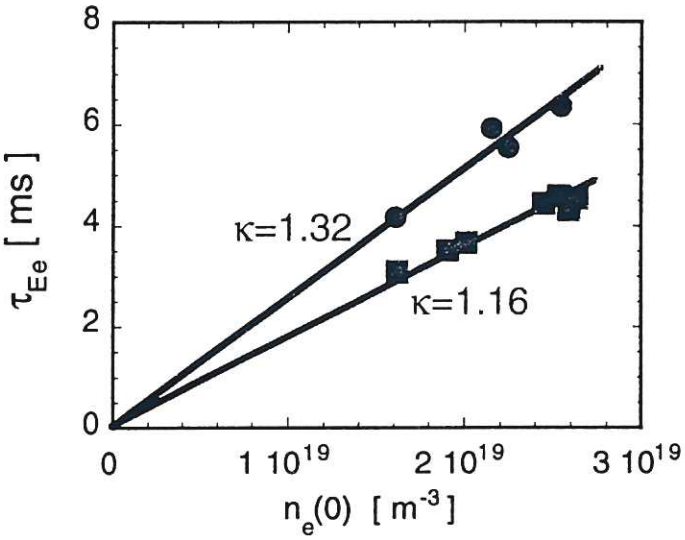
8
6
4
2
0
τ_{Ee} [ms]
κ=1.32
κ=1.16
0
1 10^{19}
2 10^{19}
3 10^{19}
$n_e(0)$ [m^{-3}]

(b)

Fig 4

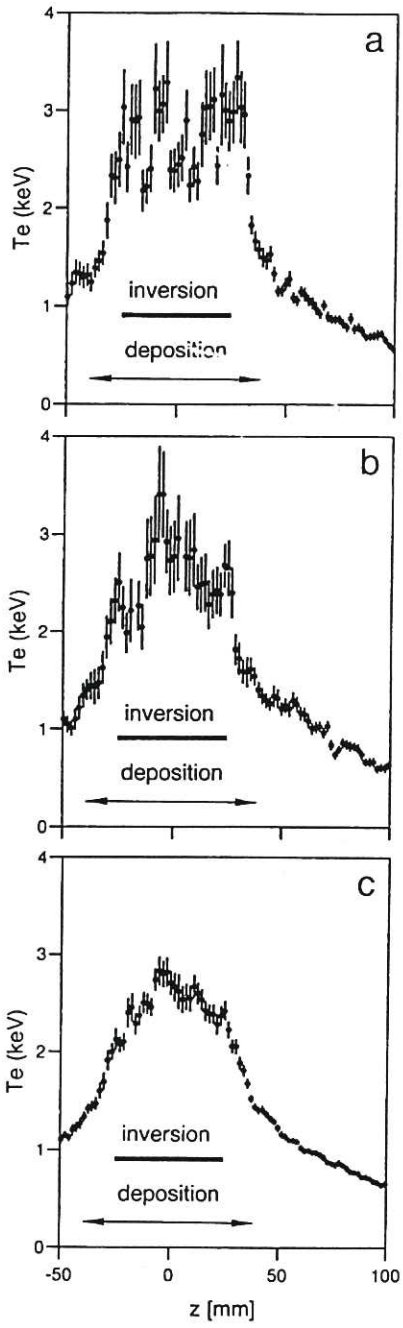

Fig 5

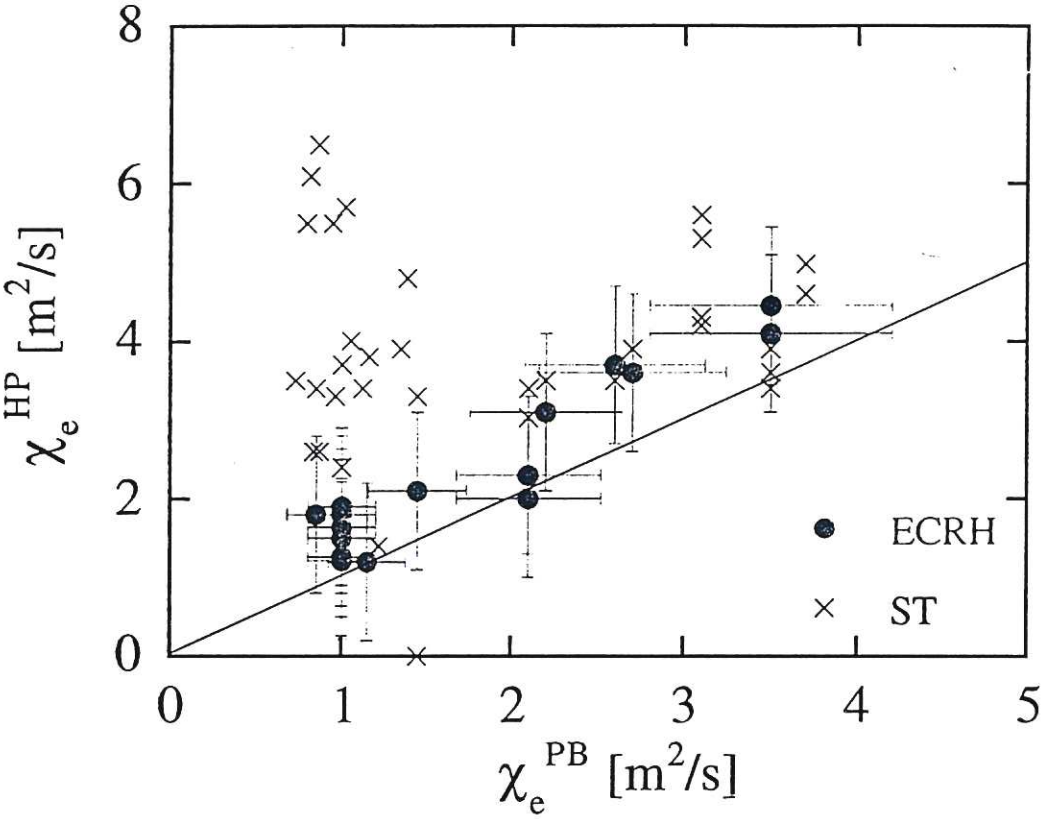

Fig 6

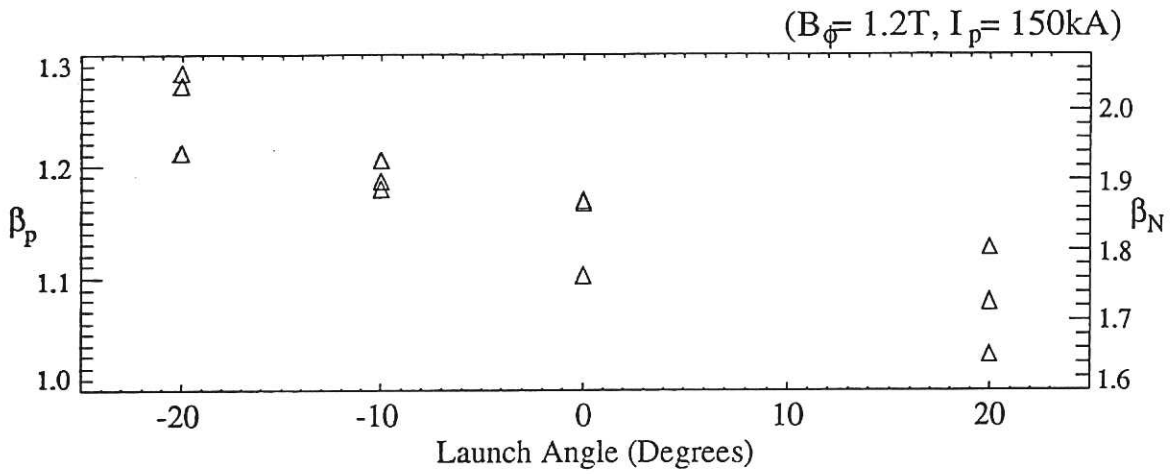
(B_ϕ= 1.2T, I_p= 150kA)
1.3
1.2
1.1
1.0
β_p
2.0
1.9
1.8
1.7
1.6
β_N
-20
-10
0
10
20
Launch Angle (Degrees)

(a)

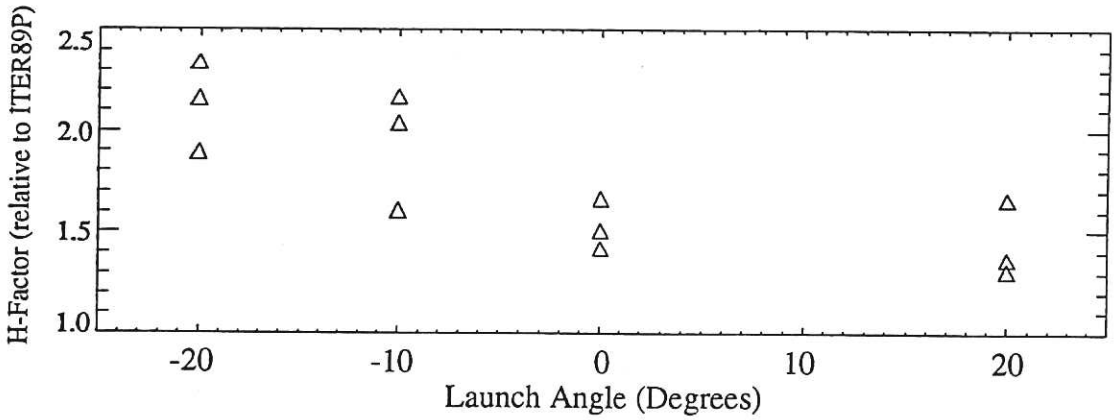
H-Factor (relative to ITER89P)
2.5
2.0
1.5
1.0
-20
-10
0
10
20
Launch Angle (Degrees)

(b)

Fig 7

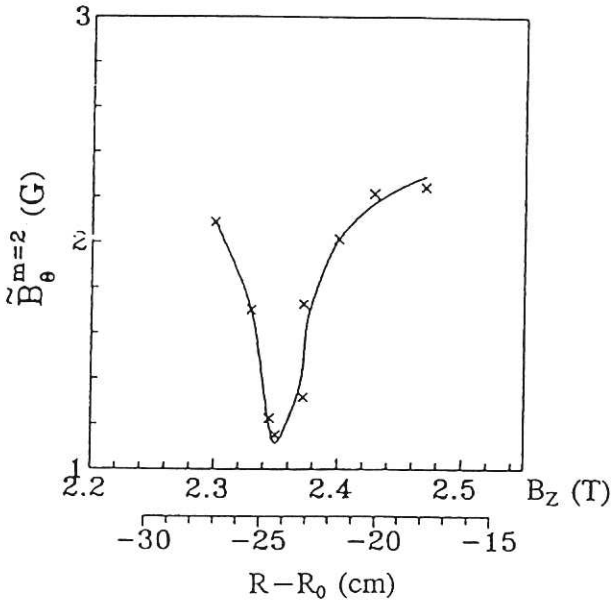
3
2
1
$\tilde{B}_\theta^{m=2}$ (G)
2.2
2.3
2.4
2.5
B_Z (T)
−30
−25
−20
−15
R−R₀ (cm)

(a)

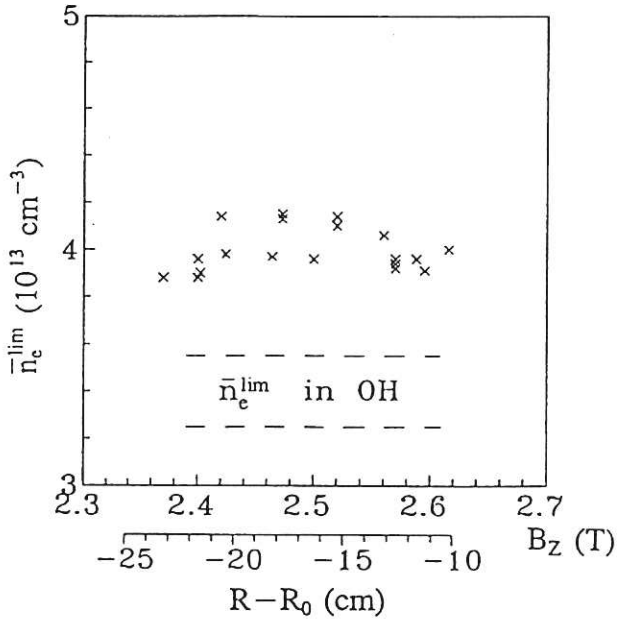
5
4
3
$\bar{n}_e^{lim}$ (10^{13} cm^{-3})
$\bar{n}_e^{lim}$ in OH
2.3
2.4
2.5
2.6
2.7
B_Z (T)
−25
−20
−15
−10
R−R₀ (cm)

(b)

Fig 8

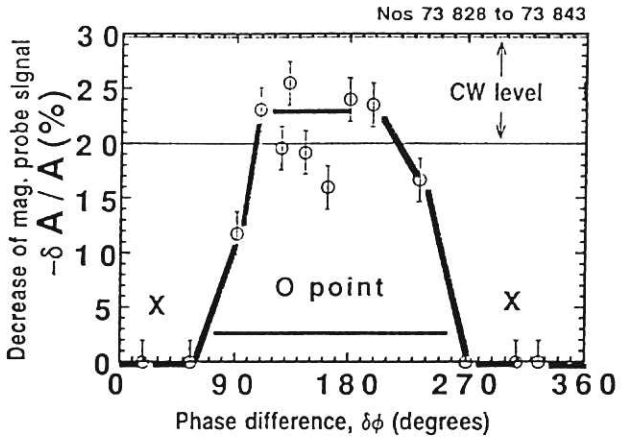
Nos 73 828 to 73 843
Decrease of mag. probe signal
-δ A / A (%)
30
25
20
15
10
5
0
CW level
O point
X
X
0
90
180
270
360
Phase difference, δφ (degrees)

Fig 9